Fine Tuning of Physical Properties of Designed Polypeptide Multilayer Films by Control of pH

ARTICLE *in* BIOTECHNOLOGY PROGRESS · FEBRUARY 2006

Impact Factor: 2.15 · DOI: 10.1021/bp050130h · Source: PubMed

3 AUTHORS, INCLUDING:

Bingyun Li
West Virginia University
58 PUBLICATIONS **1,033** CITATIONS

Fine Tuning of Physical Properties of Designed Polypeptide Multilayer Films by Control of pH

Yang Zhong, Bingyun Li,† and Donald T. Haynie*

Biomedical Engineering and Physics, Bionanosystems Engineering Laboratory, Center for Applied Physics Studies, Louisiana Tech University, PO Box 10137, Ruston, Louisiana 71272

Adjustment of pH can alter the ensemble of three-dimensional structures of a polypeptide in solution by changing the distribution of charge and Coulombic interactions. The role of pH in layer-by-layer self-assembly (LbL) of designed 32mer peptides containing the amino acid cysteine has been investigated using a combination of physical methods. Results show that pH can have a substantial influence on the mass of adsorbed peptide, surface roughness, and film density over a range of 1.5 pH units. Peptide film thickness depends on the number of layers, as with "conventional" polyelectrolytes. Film density and morphology, however, vary more with pH than does thickness, translating into a change in density on the order of 70% over the pH range 7.4−8.9. Results of this work provide insight on the physical basis of LbL and suggest that peptides are a promising class of polyelectrolytes for the creation of designer thin films for applications in biotechnology and other areas.

Introduction

Peptides and proteins constitute one of four basic classes of biological macromolecule. These extraordinary polyelectrolytes, alone or in aggregate form, serve as nanoscale machines in the synthesis of organic molecules, building blocks of tissue, vehicles for gas transport, and chemical effectors of development and growth in living organisms. In biotechnology, surface modification with proteins or peptides is of considerable interest for different applications, for example, membranes, biosensors, and implants (*1*−*3*). The interaction of biomolecules and cells with an implant depends on not only topology and roughness of the surface but also chemical composition (*4*). Self-assembled peptide scaffolds have imaginatively been proposed for the development of three-dimensional cell culture and tissue engineering (*5*).

Different approaches are taken in the self-assembly of molecules into films and related structures. Examples include Langmuir−Blodgett deposition (*6*, *7*), sol−gel entrapment (*8*), covalent binding (*9*), spontaneous adsorption from solution (*10*, *11*), and polyelectrolyte (PE) LbL. The last of these is attractive to biotechnology for several reasons. LbL is simple−one can make a film from PEs in aqueous solution−and it is versatile with respect to incorporation of specific chemical functionalities (*12*, *13*). Moreover, films prepared by LbL can feature nanometer-scale organization, controlled thickness, and designed supramolecular architecture. The ability to build a "nanofilm" from peptides in a predetermined way therefore seems promising for the development of applications in biotechnology, medicine, and other fields.

Material properties of an LbL film can be manipulated in different ways. Variables include choice of substrate, solution conditions, method of post-fabrication functionalization, and PE structure. The mean charge per unit length of a "weak" PE varies gradually with pH. Polypeptides are considered weak PEs. Experimental multilayer film studies involving "conventional" weak PEs, for instance, poly(allylamine hydrochloride) and poly(acrylic acid), have revealed that various film properties can depend strongly on the pH of the polyelectrolyte assembly solution. Examples include surface friction, roughness, film morphology, and dielectric properties (*14*−*19*). pH can be used to "tune" film thickness (*15*, *20*−*23*), polymer interpenetration and surface wettability (*14*), film stability and morphology (*16*, *25*−*29*), and permeability (*24*, *30*) when PEs are weak. The effect of solution pH on weak PE multilayer film assembly has also been studied theoretically (*31*).

Despite extensive work on weak PE multilayers, further study should be devoted to polypeptide films for at least two reasons: the properties of a film and therefore its suitability for an application, particularly in a biological context, could depend essentially on chemical properties of peptides versus some other type of weak PE, and it should not be assumed that all polypeptides, particularly designed peptides, will behave in ways that can be predicted from the known properties of a handful of well-studied weak PEs or even the known properties of poly(L-lysine) (PLL) and poly(L-glutamic acid) (PLGA).

Previous work in our laboratory has characterized self-assembly of polypeptides and various properties of the resulting multilayer films. We have shown, for instance, that pH can be used to the control assembly of PLL and PLGA in the range pH 4−10 and the secondary structure content of PLL/PLGA films following fabrication at neutral pH (*29*, *32*). We have found that peptides designed according to a few basic principles can be suitable for LbL, even when the molecular weight is as low as ∼3500 Da (*33*, *34*), and we have shown that films of cysteine-containing peptides have increased resistance to degradation at acidic pH on formation of disulfide bonds (*34*).

Here, quartz crystal microbalance (QCM), UV−visible wavelength spectroscopy (UVS), circular dichroism spectrometry (CD), and ellipsometry have been used to monitor the

* To whom correspondence should be addressed. Tel: +1 (318) 257-3790. Fax: +1 (318) 257-2562. Email: haynie@latech.edu.

† Present address: Department of Orthopedics, West Virginia University School of Medicine, PO Box 9196, Morgantown, WV 26506.

10.1021/bp050130h CCC: $33.50
Published on Web 08/11/2005

adsorption of designed 32mer peptides onto various types of solid support (QCM resonators, quartz slides, Si wafers). Film thickness has been assessed by ellipsometry and surface profilometry. Atomic force microscopy (AFM) has been used to characterize surface morphology. Results indicate that smooth and dense polypeptide multilayer films or comparatively rough and loose-packed ones can be prepared from 32mers by adjusting solution pH over a range of just 1.5 pH units near neutral pH. We have also found that adjustment of solution pH influences surface roughness, thickness, and refractive index (RI) of multilayer films of these peptides in distinct ways from conventional PEs and long homopolypeptides.

Experimental Section

In earlier work two 32mer peptides were designed to contain cysteine and to have a high density of positive charge or a high density of negative charge at neutral pH:

(1) KVKG/KCKV/KVKG/KCKV/KVKG/KCKV/KVKG/KCKY

(2) EVEG/ECEV/EVEG/ECEV/EVEG/ECEV/EVEG/ECEY

where K, E, V, G, C, and Y represent lysine, glutamic acid, valine, glycine, cysteine, and tyrosine, respectively (*34*). The design rationale was as follows. In Peptide 1, K is for electrostatic attraction to a negatively charged surface, V for hydrophobicity, G for polypeptide backbone flexibility, and C for reversible disulfide bond formation. In Peptide 2, E is for electrostatic attraction to a positively charged surface. In both cases Y, which is aromatic, is for spectroscopic detection and quantification of peptide concentration. A large increase in film stability can be achieved with these peptides by disulfide bond formation (*34*), and their average net charge varies more or less predictably with pH (see below) (*35*).

The present study has investigated the role of solution pH on deposition of Peptides 1 and 2 and physical properties of the resulting films. Peptide concentration was 2 mg/mL in 10 mM Tris-HCl buffer, 20 mM NaCl, and 10 mM DTT. pH was 7.4, 7.8, or 8.9. Tris buffers throughout this range and was used in all experiments. The range pH 7.4−8.9 was chosen for two reasons: the cysteine side chain titrates in this region, and use of the same buffer reduces variables, simplifying interpretation of results. The rinsing solution for samples prepared on QCM resonators or quartz microscope slides contained 10 mM Tris-HCl and 20 mM NaCl, and the pH matched that of the assembly buffer. The presence or absence of DTT, a reducing agent, in the rinsing solution had no effect on film assembly (data not shown). ⟨100⟩ Si wafers of 1.4 nm average SiO_2 thickness were used for ellipsometry, surface profilometry, and AFM experiments. Wafers were cleaved into 10 × 25 mm^2 rectangles in a clean room with fewer than 100 particles larger than 0.5 μm per cubic foot of air space (class 100), rinsed with deionized water, dried with nitrogen gas, and sealed in dust-free vials. The average value of at least three measurements at ambient temperature was obtained in QCM, ellipsometry, and profilometry experiments. Further information on materials used, the film assembly process, QCM, and CD is available in Supporting Information and ref 36.

Absorption spectra of peptide multilayer films deposited on quartz microscope slides were recorded at ambient temperature in the wavelength range 190−300 nm with a Shimadzu UV-1650 PC UV−vis spectrophotometer (Japan). Background information on ellipsometry and the underlying theory is available in various sources (*37*−*41*). Here, a four-layer optical layer model (Si substrate/SiO_2/peptide film/ambient air) was used to determine mean values of RI and average film thickness from the measured ellipsometric angles, ψ and Δ, with a Sentech SE 850 instrument (Germany). The angle of incidence was 70°. Measurements were made on dry films at ambient temperature. It was assumed that the films were homogeneous and isotropic; this obvious simplification could have some bearing on the measured values. Film thickness was also determined in contact mode using an Alpha-Step IQ surface profiler (KLA Tencor Corporation, USA). A peptide film was gently scratched, and the scratch was profiled with a diamond stylus tip. The force was 16.2 mg, scan length 400 μm, speed 5 μm/s, sampling rate 50 Hz, and sensor range 20 μm/1.19 pm. Surface scanning experiments were done at ambient temperature in tapping mode using a Q-scope 350 scanning probe microscope (Quesant Instrument Corp., USA). Scanning rate was 2 Hz, resolution 500 pixels (20 μm × 20 μm images) or 1000 pixels (1μm × 1 μm images).

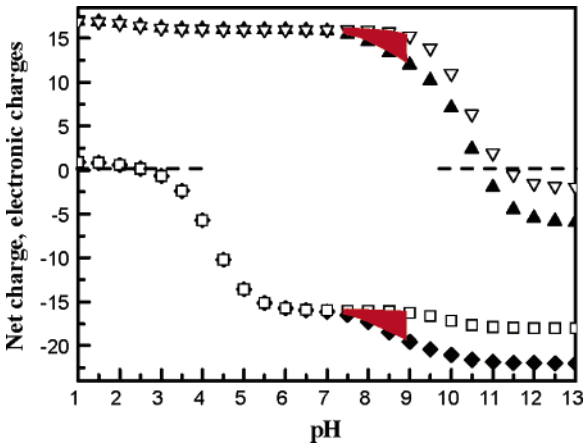

Figure 1. Calculated net charge versus pH. Shaded regions indicate range of values discussed in this work. Triangles: Peptide 1. Squares: Peptide 2. Solid symbols: Peptides 1 and 2 as studied here. Open symbols: Peptides 1 and 2 with cysteine replaced by serine.

Results

Peptide 1 and Peptide 2 are weak PEs. The linear charge density of the peptides, however, will be high throughout the pH range 7.4−8.9 (Figure 1) (*35*). This is because the intrinsic pK_a's of Lys and Glu, respectively, 10.5 and 4.3, are outside the range of interest here; normally both side chains are charged at neutral pH, even in unstructured polymers and proteins, and complex formation between PLL and PLGA will shift the pK_a's away from neutral. By contrast, thiol titrates in the range 7.4−8.9. An increase in pH from neutral therefore will decrease the net charge on Peptide 1 and increase it on Peptide 2 (Figure 1). A single Peptide 1 molecule thus will have both positive and negative side chains at pH 8.9, increasing the odds of intramolecular salt bridge formation and aggregation. In Peptide 2 the side chains of Glu will repel those of Cys when the latter become ionized, increasing chain stiffness. The absolute net charge of Peptides 1 and 2 is matched at pH 7.4, but disparity grows with increase in alkalinity (Figure 1). It was suspected that changes in peptide charge density would have some impact of film assembly. Experiments described here were done to determine the general character and magnitude of change.

UV absorbance of quartz slides increased and resonant frequency of QCM resonators decreased with adsorption step during peptide self-assembly (Figure 2a). This was expected from the previous studies on "conventional" PEs and peptides

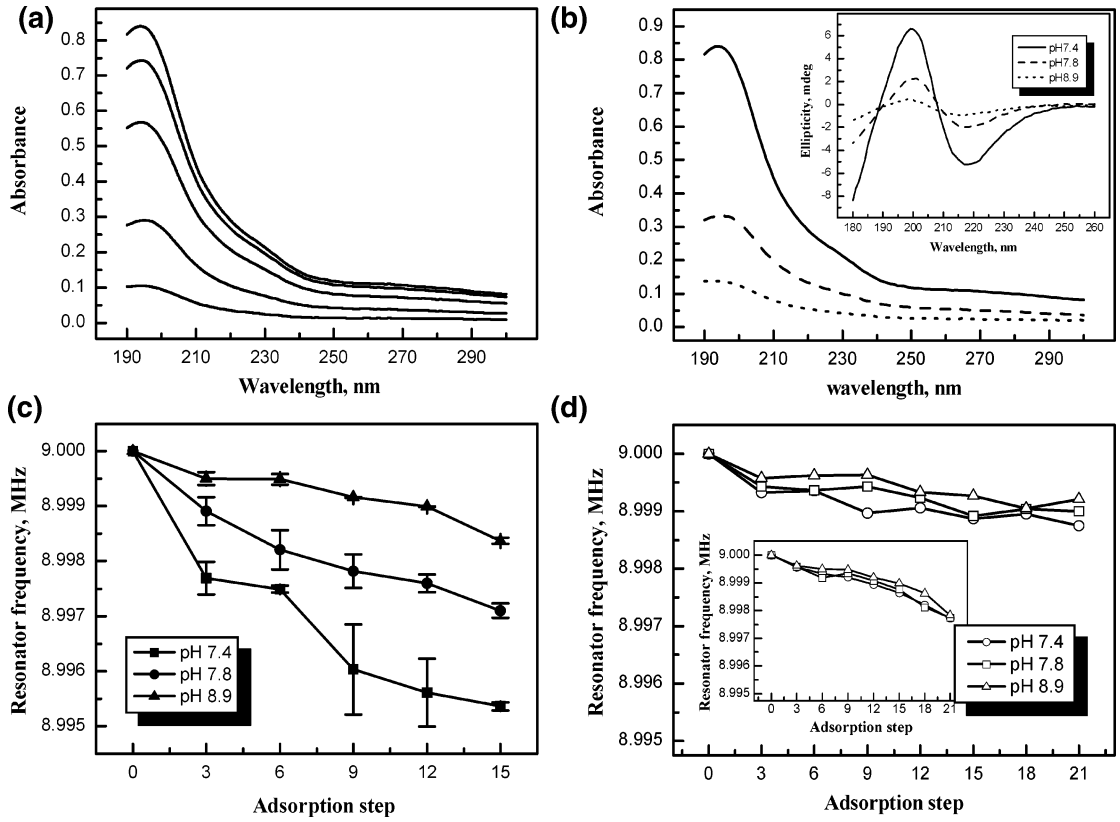

Figure 2. pH dependence of peptide multilayer film preparation. Error bars represent standard deviations. (a) UV−vis. Spectra were collected after deposition of 3, 6, 9, 12, or 15 layers. Films were otherwise treated in the same way after each adsorption step. Absorbance increased with the number of layers. (b) Comparison of UV−vis and CD (inset) for 15-layer films. (c) QCM. Resonant frequency decreased with number of layers of short designed peptide, indicating deposition of material. Frequency shift depends substantially on pH. (d) QCM. Resonant frequency decreased with number of layers of 32mers of PLL and PLGA or (inset) 13.6 kDa PLL and 14.6 kDa PLGA, indicating deposition of material. Frequency shift is practically independent of pH.

cited above. For Peptide 1 and Peptide 2 at pH 7.4, absorbance was about 0.056 AU/layer at 194 nm (Figure 2b) and frequency shift about −310 Hz per adsorption step near 9 MHz (Figure 2c), the nominal resonant frequency of the resonators. Not predicted was the 30−80% decrease in adsorption of these peptides detected by UVS (Figure 2b), CD (Figure 2b), and QCM (Figure 2c) on increasing the pH by just 1.5 units (Table 1). PLL and PLGA have an approximately constant charge per unit length in the range pH 7.4−8.9, because neither lysine nor glutamic acid titrates in this region, and these peptides exhibit similar assembly behavior under these conditions (Figure 2d).

CD has revealed that Peptide 1/Peptide 2 films have a large content of β sheet (Figure 2b inset). The negative Cotton effect at ca. 216 nm and the positive one at ca. 197 nm provide the necessary evidence for secondary structure content (*42*). This is consistent with our previous study of the designed peptides (*36*) and similar to the secondary structure content of PLL/PLGA films (*29*). There was some conformational change in peptides in the film, but apparently little, on change of pH in the range 7.4−8.9; a structural transition will result in a corresponding change in the shape of the spectrum (*42*).

Ellipsometry has shown that film thickness increases with number of adsorption steps (Figure 3a). Surprisingly, thickness at pH 8.9 was about the same as at pH 7.4, despite the apparent difference in deposited mass (Figure 2b and c). Surface profilometry measurements (Figure 3b) corroborated ellipsometry, in most cases to within 15% (Table 2). Ellipsometric RI varied with adsorption step, from 1.58 to 1.65 over a range of thickness of 20−60 nm, similar to protein films in air (see below); the opposite trend was found for film disassembly. RI was higher for samples deposited at pH 7.4 than 8.9 (Figure 3c). This difference, however, was always less than 2% and decreased with increasing layers.

Table 1. Film Mass Measurements[a]

	% difference		
pH	by UVS	by QCM	by CD
7.4	0	0	0
7.8	−60	−38	−61
8.9	−84	−65	−80

[a] Adsorbed mass for 15 layers was measured by change in photon absorbance (UVS), change in resonant frequency (QCM), and change in ellipticity (CD). Differences between the optical methods and QCM may have to do with the character of the surface onto which the peptides were adsorbed. Films for UVS and CD were prepared on quartz microscope slides, and the consistency of results is very good. Silver-coated quartz resonators were used for QCM measurements.

Figure 4 displays AFM images of the surface morphology of 40-layer Peptide 1/Peptide 2 films. Evidently, contaminant particles were on the surface of unmodified wafers (Figure 4d), despite preparation in a class 100 clean room. Nevertheless, films fabricated at pH 7.4 were relatively smooth (Figure 4c), whereas ones prepared at pH 8.9 were comparatively rough (Figure 4a). Films made at pH 7.8 had an intermediate roughness (Figure 4b). Essentially the same result was obtained with independently prepared 20-layer films (see Supporting Information). The vertical scales of the AFM images (legend of Figure 4) give an approximate quantitative measure of surface roughness and dependence on pH.

Discussion

Peptides 1 and 2 were known to be suitable for multilayer film formation at neutral pH prior to the study described here

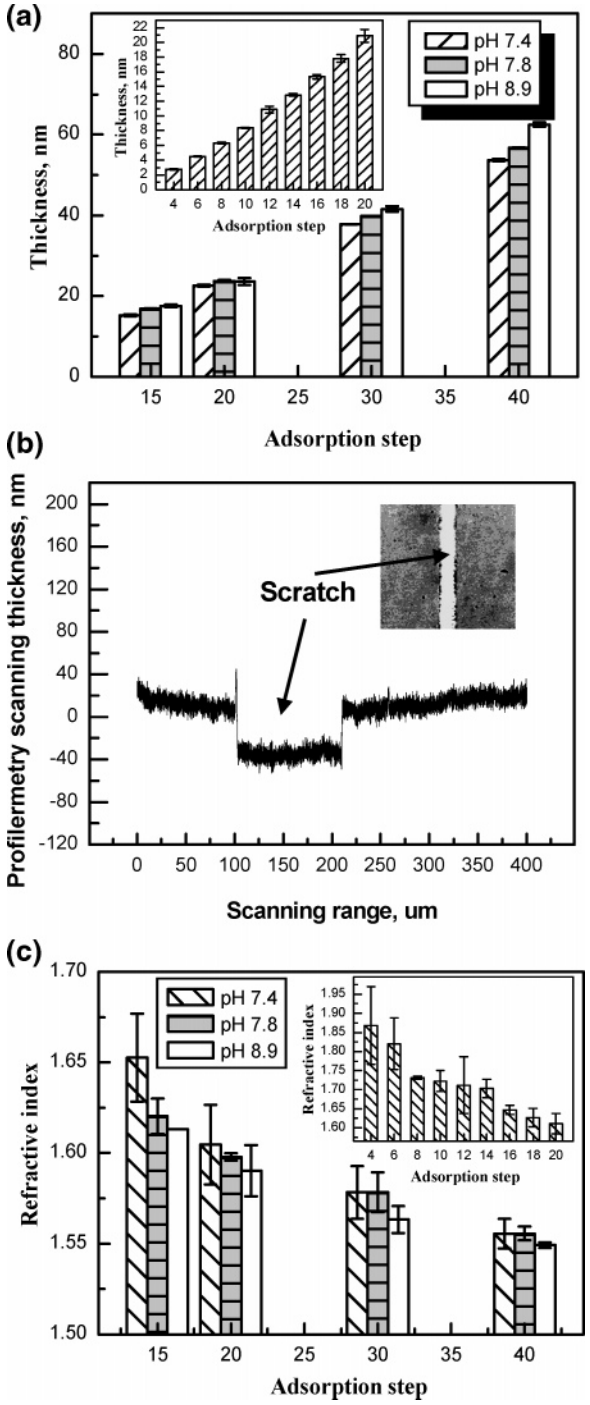

Figure 3. Bulk film thickness and surface properties. (a) Peptide 1/Peptide 2 film thickness versus adsorption step measured by ellipsometry. (b) Typical surface profilometry scanning profile over a scratch on a Peptide 1/Peptide 2 film sample. At least three thickness measurements were made for each of the data points in (a). Inset shows the position of the scratch on the film. (c) RI of peptide multilayer films determined by ellipsometry. The value after 20 layers (∼1.6) is close to that of protein films measured in air.

(*34*). The present work has revealed that a small adjustment in pH can lead to a substantial difference in the assembly behavior of these peptides and physical properties of the corresponding films. The 1.5 unit pH range was chosen to test the effect of ionization of cysteine on polymer assembly and film properties.

In broad terms results presented here resemble previous work on PLL and PLGA (*29*, *34*) and on "conventional" polyelectrolytes (*16*, *25*−*28*). Comparison of the behavior of Peptide 1/Peptide 2 and PLL/PLGA under identical conditions, however, would suggest that predicting the assembly behavior of weak PEs and the physical properties of the resulting films will be difficult on the basis of chemical structure alone: predicting the assembly behavior of polypeptides and the properties of the corresponding films is akin to solving the protein folding problem.

Figure 2a shows variation in UVS signal with adsorption step on assembly of Peptides 1 and 2. The monotonic increase in signal implies that peptide was deposited during each step of the fabrication process. Both UVS (Figure 2b) and CD (Figure 2b), optical methods, and QCM (Figure 2c), a mechanical method, indicated that pH has a substantial effect on assembly of Peptides 1 and 2 in the range 7.4−8.9. "Mass" measurements by these methods are compared in Table 1. If any of the change in UVS signal is attributable to conformational change of peptide bonds, it must be small according to CD. By contrast, neither 32mers of PLL and PLGA nor larger versions of these peptides exhibited an obvious dependence on pH in the indicated range (Figure 2d), as expected from earlier study of PLL and PLGA films (*29*, *34*) and related reports (*43*, *44*).

Peptide 1, Peptide 2, PLL and PLGA are weak PEs. Why, then, does their assembly behavior differ? Charge density depends on pH. At pH 7.4, the absolute value of the net charge on Peptides 1 and 2 is matched; the linear charge density is about the same (Figure 1). The same is true of PLL and PLGA, though the linear charge density, close to 1, is about twice that of Peptides 1 and 2. The similarity in charge density may allow Peptides 1 and 2 to form tight complexes at neutral pH, all charges being compensated in the peptide film. Because Peptides 1 and 2 are relatively short and the linear charge density is relatively high at neutral pH, they closely approximate rigid rods under these conditions. 32mers of PLL and PLGA will be even stiffer at neutral pH, given the higher charge density.

As the pH becomes increasingly alkaline, cysteine deprotonates; its pK_a is near 8.4. At pH 8.9, then, Peptide 2 is more extensively ionized and has a higher net charge than at pH 7.4. Peptide 1 must have a lower net charge (Figure 1, inset). The increase in net charge of Peptide 2, though modest, will lead to a change in the ensemble of conformations in solutions, as the like-charged side chains of glutamic acid and cysteine will repel each other and influence backbone structure and chain stiffness. Thiolate will contribute to the overall electrostatic potential of the peptides and thus alter their tendency to adsorb onto a charged surface and the mechanisms of intermolecular interaction during and after adsorption. Peptide 1 has positively charged lysine and negatively charged cysteine side chains at pH 8.9. Oppositely charged residues within a single peptide molecule will attract each other to some extent, biasing peptide conformation in solution or in the film. The pH-based mismatch in charge between Peptides 1 and 2 could potentially influence the cooperative association of peptides (*45*) and the rate and extent of diffusion of molecules in the film (*46*). By contrast, the adsorption behavior of PLL and PLGA showed no dependence on pH in the range pH 7.4−8.9, reflecting marginal change in average molecular charge and chain stiffness under these conditions.

Peptide 1/Peptide 2 film thickness has been studied by ellipsometry and profilometry. Figure 3a shows that ellipsometric film thickness at pH 8.9 was about the same as at pH 7.4, despite the significant dependence of mass deposition on pH. Surface profilometry experiments have confirmed the ellipsometry data. Measured thickness was a few percent smaller by surface profilometry than by ellipsometry, presumably because the former is a contact mode method, requiring a stylus

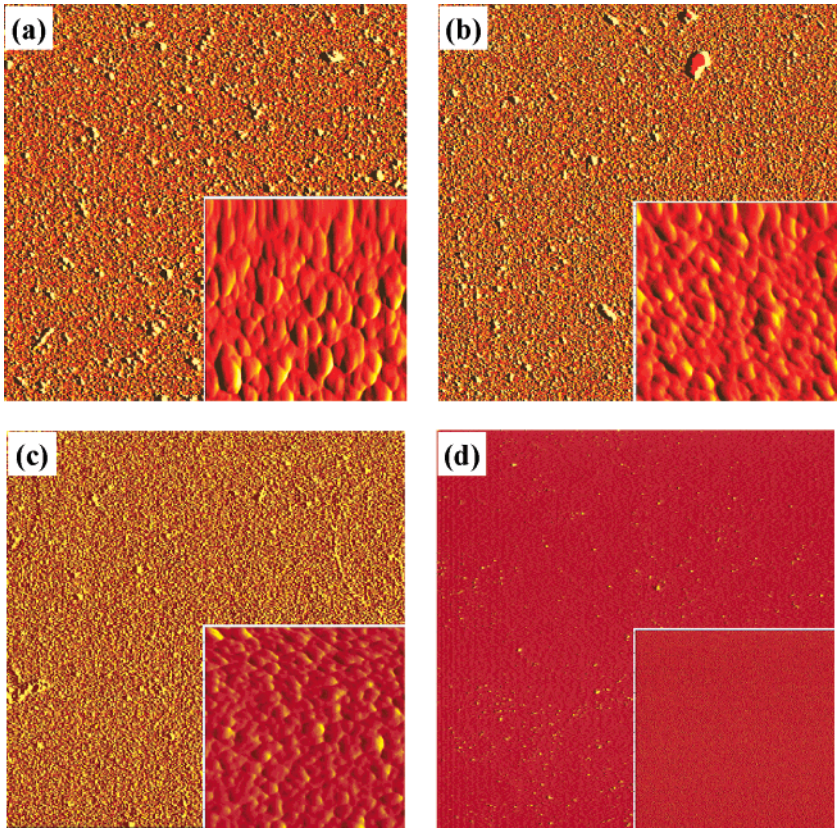

Figure 4. AFM micrographs of 40-layer peptide films deposited at different pH values, 20 μm × 20 μm and 1 μm × 1 μm (insets). (a) pH 8.9, (b) pH 7.8, (c) pH 7.4, and (d) Si wafer. Vertical scales are 194, 150, 84, and 36 nm, respectively, for 20 μm × 20 μm, and 34, 29, 27, 15, respectively, for 1 μm × 1 μm. Some of the surfaces cannot be visualized if the same vertical scale is used throughout.

Table 2. Film Thickness Measurements[a]

	20 layers					40 layers				
pH	SP (nm)	% diff	E (nm)	% diff	% diff between methods	SP (nm)	% diff	E (nm)	% diff	% diff between methods
7.4	19.8 ± 0.3	0	22.6 ± 0.3	0	14	49.4 ± 0.3	0	53.7 ± 0.2	0	9
7.8	18.3 ± 0.6	−8	23.8 ± 0.2	5	30	54.2 ± 1.8	10	56.8 ± 0.1	6	5
8.9	21.3 ± 0.4	8	23.6 ± 0.9	4	11	59.2 ± 0.8	19	62.5 ± 0.6	16	6

[a] Thickness is in nanometers, measured by surface profilometry (SP) and ellipsometry (E), of 20- and 40-layer peptide films prepared at different pH values. Error bars represent standard deviations.

force, and the latter is a noncontact mode method. QCM showed that the mass deposited was about three times higher at pH 7.4 than at 8.9 for a 15-layer peptide film (Figure 2c) (*3*, *47*). Taken together, the deposition and thickness measurements would suggest that film density was considerably higher at pH 7.4 than at 8.9. If so, Peptides 1 and 2 may pack onto the surface with a lower degree of order at pH 8.9 than at 7.4, a small amount of loosely packed material at the higher pH occupying about the same volume as a large amount of densely packed material at the lower pH. It would follow that greater mass deposited does not necessarily imply greater film thickness, as is often assumed in the study of conventional PEs.

AFM experiments have revealed that films of Peptides 1 and 2 formed at pH 7.4 have a relatively smooth surface. The vertical axis scales in Figure 4 are 194 nm for pH 8.9, 150 nm for pH 7.8, and 84 nm for pH 7.4. The character of the film at pH 7.4 is consistent with dense packing. It would appear that molecules are distributed essentially uniformly on the flat substrate, forming somewhat "homogeneous" layers. Surface roughness at pH 8.9 was substantially greater than at pH 7.4, indicating differences in peptide interaction. It may be that the heterogeneity of peptide conformation is greater at the elevated pH, leading to decreased surface smoothness. In any case, it is evident that adjusting the pH in a narrow range can induce a significant change in peptide LbL film properties in a way that could hardly be predicted on the basis of the behavior of PLL and PLGA.

Previous studies have shown that solution pH can have a dramatic effect on weak polyion adsorption behavior over a narrow pH range (*14*−*19*). Control of pH has been used to control layer thickness. For instance, a remarkable transition in thickness, from 45 to 3 Å layer^{-1}, has been reported by the Rubner group over a pH range of just 0.5 units in the PAA/PAH system (*14*). In a separate study, pH shift from 7.4 to 5.0 altered the adsorption properties of human serum albumin (*48*), presumably by changing the net charge of the molecule. Here, change in thickness of designed polypeptide multilayer films was relatively small in the range pH 7.4−8.9, despite the rather substantial dependence of material adsorbed on pH. Why a difference in behavior?

The designed peptides are short, nearly monodisperse heteropolymers, whereas those studied by the Rubner group are long, polydisperse homopolymers. Human serum albumin, a protein, has a rough and complex surface structure in the folded state, more complex than the structure of an individual Peptide

1 or 2. The data show that Peptide 1/Peptide 2 films of relatively smooth surface and high density or rough surface and loose packing can be fabricated by slight adjustment of pH. The ability to control such physical properties of polypeptide films could be useful in the development of specific applications, for example, the membrane-based enantiomeric separations reported by the Schlenoff group (*30*), controlled release of encapsulated pharmacological agents, or surfaces for tissue culture.

pH has been used to tune RI in the development of antireflective coatings (*18*). Here, surface roughness of dry films increased as pH increased from 7.4 to 8.9. This correlates with an observed decrease in RI (Figure 3c). It also resembles the increase in RI with concentration of protein in solution (*37*). The RI data thus are consistent with the view that the density of dry Peptide1/Peptide 2 films is higher at pH 7.4 than 8.9, and they are consistent with the results of independent studies that have shown that RI is 1.35−1.6 for adsorbed protein layers (*49*, *50*) and 1.53−1.66 for 20-layer PAH/poly(styrenesulfonate) (*15*).

The measured RI value could depend on interference, anisotropy, order and packing (*51*), possible differences in optical properties of the adsorbing polymers (*52*), differences in molecular surface area (*53*), number of bilayers (*54*), amount of water present (*55*), and model adopted for analysis. The multilayer films prepared in the present work consisted of two oppositely charged peptides, water, and salt. Film structure was complex, comprising not only different molecular conformations but in fact different types of secondary structure. The distribution of secondary structures in peptides in solution will depend on pH as will the amount of material deposited, even if the average structure in solution is a random coil, because the net charge on a molecule depends on pH. In any case, the polypeptide films are hardly perfectly homogeneous and isotropic, as assumed in analysis.

A decrease in RI with increasing thickness has been found in independent studies. For example, in work by Wang and Chang pH-induced increases in thickness of surface-tethered PLL and PLGA corresponded not only to a helix-coil transition in the film, detected by CD, but also to a decrease in RI (*56*). Plasma-polymerized di(ethylene glycol)monovinyl ether films have a RI that depends on film density (*57*). Mesoionic side chain methacrylate polymers show a continuous decrease in RI with increase in film thickness, which could be due to the reduction in molecular polarizability from loss of conjugated double bonds and the increase of volume (*58*). In view of this, the variation of RI with conditions in the case of Peptide 1/Peptide 2 does not seem very unusual, even if it is not clear why RI varies. Substrate surface may influence parameter determination, particularly when the layer number is small, so film thickness may need to be considered when attempting to infer structural information such as layer thickness from optical measurements using an assumed RI.

Conclusions

Combining different approaches, e.g., QCM, UVS, CD, ellipsometry, surface profilometry, and AFM, all label-free methods, can provide a substantially more comprehensive view of polypeptide film properties than a single technique. Solution pH can have a substantial effect on polypeptide multilayer film thickness, density, surface morphology, and RI in the case of designed peptides. PE film density cannot be assumed constant under different conditions. It would appear that the ionization state of Cys side chains plays a key role in the observed peptide adsorption behavior. The assembly behavior of the designed polypeptides and physical properties of the corresponding multilayer films could not have been predicted on the basis of better-known properties of PLL and PLGA. Polypeptide multilayer films could be used as artificial biomembranes or for biomaterials surface modification.

Acknowledgment

We thank Karen Xu for helpful discussions and assistance with AFM and surface profilometry experiments and Satish Bharadwaj and Ling Zhang for helpful comments on this work. This research was supported in part by a Nanotechnology Exploratory Research award from the National Science Foundation (DMI-0403882), a seed grant from the Center for Entrepreneurship and Information Technology, and the 2002 Capital Outlay Act 23 of the State of Louisiana (Governor's Biotechnology Initiative).

Note Added at Proof. Similar behavior of refractive index versus layer number has been found for multilayer films of PLL and PLGA by Halthur et al. *J. Am. Chem. Soc.* **2004**, *126*, 17009.

Supporting Information Available: Procedure used in QCM and CD experiments and AFM micrographs of the surface of 20-layer peptide films deposited at different pH values. This material is available free of charge via the Internet at http://pubs.acs.org.

References and Notes

(1) Lvov, Yu.; Ariga, K.; Kunitake, T. *Chem. Lett.* **1994**, 2323.
(2) Caruso, F.; Furlong, D. N.; Ariga, K.; Ichinose, I.; Kunitake, T. *Langmuir* **1998**, *14*, 4559.
(3) Lvov, Yu.; Ariga, K.; Ichinose, I.; Kunitake, T. *J. Am. Chem. Soc.* **1995**, *117*, 6117.
(4) Mrksich, M.; Whitesides, G. M. *Annu. Rev. Biophys. Biomol. Struct.* **1996**, *25*, 55.
(5) Zhang, S. *Nat. Biotechnol.* **2003**, *21* (10), 1171.
(6) Turko, I. V.; Yurkevich, I. S.; Chashchin, V. L. *Thin Solid Films* **1991**, *205*, 113.
(7) Dubrovsky, T.; Vakula, S.; Nicolini, C. *Sens. Actuators, B* **1994**, *22*, 69.
(8) Avnir, D.; Braun, S.; Lev, O.; Ottolengthi, M. *Chem. Mater.* **1994**, *6*, 1605.
(9) Leggett, G. J.; Roberts, C. J.; Williams, P. M.; Davies, M. C.; Jackson, D. E.; Tendler, S. J. B. *Langmuir* **1993**, *9*, 2356.
(10) Lin, J. N.; Drake, B.; Lea, A. S.; Hansma, P. K.; Andrade, J. D. *Langmuir* **1990**, *6*, 509.
(11) Wahlgren, M.; Arnebrant, T. *J. Colloid Interface Sci.* **1993**, *142*, 503.
(12) Tripathy, S. K.; Kumar, J.; Nalwa, H. S. *Handbook of Polyelectrolyte-Based Thin Films for Electronic and Photonic Applications*; American Scientific Publishers: Stevenson Ranch, CA, 2002; Vol. 1, p 1.
(13) Decher, G.; Schlenoff, J. B. *Multilayer Thin Films*; Wiley-VCH: Weinheim, Germany, 2003.
(14) Yoo, D.; Shiratori, S. S.; Rubner, M. F. *Macromolecules* **1998**, *31*, 4309.
(15) Harris, J. J.; Bruening, M. L. *Langmuir* **2000**, *16*, 2006.
(16) Mendelsohn, J. D.; Barrett, C. J.; Chan, V. V.; Pal, A. J.; Mayes, A. M.; Rubner, M. F. *Langmuir* **2000**, *16*, 5017.
(17) Fery, A.; Scholer, B.; Cassagneau, T.; Caruso, F. *Langmuir* **2001**, *17*, 3779.
(18) Hiller, J.; Mendelsohn, J. D.; Rubner, M. F. *Nat. Mater.* **2002**, *1*, 59.
(19) Burke, S. E.; Barrett, C. J. *Biomacromolecules* **2003**, *4*, 1773.
(20) Kim, B. Y.; Bruening, M. L. *Langmuir* **2003**, *19*, 94.
(21) Mermut O.; Barrett, C. J. *Analyst* **2001**, *126*, 1861.
(22) Sun, J. Q.; Wu, T.; Liu, F.; Wang, Z. Q.; Zhang, X.; Shen, J. C. *Langmuir* **2000**, *16*, 4620.
(23) Schoeler, B.; Poptoschev, E.; Caruso, F. *Macromolecules* **2003**, *36*, 5258.
(24) Sukhorukov, G. B.; Antipov, A. A.; Voigt, A.; Donath E.; Mohwald, H. *Macromol. Rapid Commun.* **2001**, *22*, 44.

(25) Hoogeveen, N. G.; Stuart, M. A. C.; Fleer, G. J.; Böhmer, M. R. *Langmuir* **1996**, *12*, 3675.
(26) Kharlampieva, E.; Sukhishvili, S. A. *Langmuir* **2003**, *19*, 1235.
(27) Hiller, J.; Rubner, M. F. *Macromolecules* **2003**, *36*, 4078.
(28) Dubas, S. T.; Schlenoff, J. B. *Macromolecules* **2001**, *34*, 3736.
(29) Zhi, Z. L.; Haynie, D. T., *Macromolecules* **2004**, *37*, 8668.
(30) Rmaile, H. H.; Farhat, T. R.; Schlenoff, J. B. *J. Phys. Chem. B* **2003**, *107*, 14401.
(31) Bohmer, M. R.; Evers, O. A.; Scheutjens, J. M. H. M*acromolecules* **1990**, *23*, 2288.
(32) Haynie, D. T.; Balkundi, S.; Palath, N.; Chakravarthula, K.; Dave, K. *Langmuir* **2004**, *20*, 4540.
(33) Zheng, B.; Haynie, D. T.; Zhong, H.; Sabnis, K.; Surpuriya, V. *J. Biomater. Sci. Polym. Ed.* **2005**, *16*, 285.
(34) Li, B.; Haynie, D. T. *Biomacromolecules* **2004**, *5*, 1667.
(35) van Holde, K. E. *Physical Biochemistry*, 2nd ed.; Prentice Hall: Englewood Cliffs, NJ, 1985; pp 77−80.
(36) Li, B.; Haynie, D. T.; Palath, N.; Janisch, D. *J. Nanosci. Nanotechnol.*, in press.
(37) Feijter, J. A. de; Benjamines, J.; Veer, F. A. *Biopolymers* **1978**, *17*, 1759.
(38) Ramsden, J. J. *Quart. Rev. Biophys.* **1993**, *27*, 41.
(39) Stalgren, J. J. R.; Eriksson, J.; Boschkova, K. *J. Colloid Interface Sci.* **2002**, *253*, 190.
(40) Azzam, R. M. A.; Bashara, N. M. *Ellipsometry and Polarized Light*; North-Holland Elsevier: Amsterdam, 1989.
(41) Cuypers, P. A.; Corsel, J. W.; Janssen, M. P.; Kop, J. M. M.; Hermens, W. T.; Hemker, H. C. *J. Biol.* Chem. **1983**, *258*, 2426.
(42) Greenfield, N.; Fasman, G. D. *Biochemistry* **1969**, *8*, 4108.
(43) Boulmedais, F.; Bozonnet, M.; Schwinté, P.; Voegel, J.-C.; Schaaf, P. *Langmuir* **2003**, *19*, 9873.
(44) Müller, M.; Kessler, B.; Lunkwitz, K. *J. Phys. Chem. B* **2003**, *107*, 8189.
(45) Zhang, L.; Li, B.; Zhi, Z.-l.; Haynie, D. T. *Langmuir* **2005**, *21*, 5439.
(46) Picart, C.; Mutterer, J.; Richert, L.; Prestwich, G. D.; Schaaf, P.; Voegel, J.-C.; Lavalle, P. *Proc. Natl. Acad. Sci. U.S.A.* **2002**, *99*, 12531.
(47) Sauerbrey, G. *Z. Phys.* **1959**, *155*, 206.
(48) Müller, M.; Rieser, T.; Dubin, P. L.; Lunkwitz, K. *Macromol. Rapid Commun.* **2001**, *22*, 390.
(49) Benesch, J.; Askendal, A.; Tengvall, P. *J. Colloid Interface Sci.* **2002**, *249*, 84.
(50) Vörös, J. *Biophys. J.* **2004**, *87*, 553.
(51) Kattner, J.; Hoffman, H. *J. Chem. Phys. B* **2002**, *106*, 9723.
(52) Ligler, F. S.; Lingerfelt, B. M.; Price, R. P.; Schoen, P. E. *Langmuir* **2001**, *17*, 5082.
(53) Ducharme, D.; Tessier, A.; Russev, S. C. *Langmuir* **2001**, *17*, 7529.
(54) Jiang, H.; Johnson, W. E.; Grant, J. T.; Eyink, K.; Johnson, E. M.; Tomlin, D. W.; Bunning, T. J. *Chem.* Mater. **2003**, *15*, 340.
(55) Wang, Y.; Chang, Y. C. *Macromolecules* **2003**, *36*, 6503.
(56) Wang, Y.; Chang, Y. C. *Macromolecules* **2003**, *36*, 6511.
(57) Zhang, Z.; Menges, B.; Timmons, R. B.; Knoll, W.; Forch, R. *Langmuir* **2003**, *19*, 4765.
(58) Bohme, F.; Klinger, C.; Menges, B.; Mittler, S.; Ritter, H.; Theis, A. *Chem. Mater.* **2002**, *14*, 2109.

Accepted for publication July 13, 2005.

BP050130H